Optical properties of cirrus clouds in the tropical tropopause region during two contrasting seasons

G S Motty[1,$,*], Malladi Satyanarayana[1,3], G S Jayeshlal[1] , V Krishnakumar[2] & V P Mahadevan Pillai[1]

[1]Department of Optoelectronics, University of Kerala, Kariavattom, Trivandrum 695 581, Kerala, India

[2]Department of Physics, St Gregorios College, Kottarakara 691 531, Kerala, India

[3]Geethanjali College of Engineering & Technology, Cheeryal (V), Keesara (M), R R Dist Hyderabad 501 301, India

[$]E-mail: mottygs@gmail.com

Radiation budget of Earth's atmospheric system is largely impacted by the presence of cirrus clouds. In order to quantify the effect of cirrus clouds, particularly in tropics, it is important to characterise its vertical structure and optical properties. The variation of the optical and microphysical properties along with the structure and dynamics of the cirrus during two contrasting seasons, the summer and the southwest monsoon over the period 2006 - 2010 were studied using the ground-based lidar measurements made at the tropical station, Gadanki (13.5°N, 79.2°E), India. The related meteorological indicators derived from radiosonde data available with Wyoming Atmospheric Data Centre were analysed .The results were compared with the data obtained from the CALIOP on board the CALIPSO satellite. Both the observations show similar pattern of seasonal variation. In most of the cirrus clouds, the top height observed was 0.8 km above and below the tropopause and top height was maximum during monsoon season. The seasonal variation of optical depth showed that most of cirrus clouds were thin and the optical depth showed highest value during monsoon period.

Keywords: Cirrus clouds, Depolarization ratio, Optical depth

PACS Nos: 42.68.Ge; 92.60.Nv

1 Introduction

Cirrus clouds are one of the most important and yet uncertain components in weather and climate studies. These high altitude clouds cover about 30% of the Earth's surface at any time[1]. Optically thin cirrus clouds usually cause positive radiative forcing at the top of the atmosphere, whereas optically thick cirrus clouds produce cooling[2]. The cloud particles show various non-spherical shapes based on their occurrence height and temperature[3] and affect the radiation budget of the Earth-atmosphere system through two opposite phenomena. Cirrus clouds scatter and reflect incoming solar radiation back to space leading to cooling of the system, which is known as the albedo effect; inversely, they absorb and partly re-emit terrestrial infrared radiation leading to warming of the system, which is known as the greenhouse effect[4]. The basic microphysical conditions, in addition to their dissimilar temperatures and altitudes in the troposphere, have fundamental implications in terms of radiative transfer[5]. Deep convection transports moist air from the ground to the upper troposphere and the air is hydrated to form cirrus clouds[6]. Thus, they play an important role in the dehydration in the tropical tropopause layer (TTL) and hence, on stratospheric humidity[6-8]. So, in order to quantify their effects on the atmosphere, the vertical structure and optical properties of these cirrus clouds are to be characterized.

The Lidar technique has become a quantitative tool for detecting and characterizing cirrus clouds and its various properties[9]. Ground-based lidar system offers an excellent way to obtain characteristic values on cirrus formations and their properties[10]. Also, the microphysical and optical properties of cirrus clouds are obtained by the lidar observations from the earth-orbiting Cloud-Aerosol Lidar with Orthogonal Polarization (CALIOP) instrument on board the Cloud Aerosol Lidar and Infrared Pathfinder Satellite Observations (CALIPSO) satellite[11]. The ground-based lidar observations could provide intensive measurements on continuous basis with high spatial and temporal resolutions, compared to the satellite observations of cirrus meant for global coverage. Utilising observations from both ground and satellite based lidars, the statistical characteristics, physical

and optical properties of cirrus clouds can be retrieved more precisely. During the last few years, significant efforts have been pursued to study the properties of cirrus clouds using the ground based lidar system over the tropical station Gadanki by Sivakumar et al.[12], Parameswaran et al.[13], and Krishnakumar et al.[14], but mainly for deriving the general features and their variations in different periods of the year. Sivakumar et al.[12] found that the thin and thick cirrus formations are closely related to the minimum tropospheric temperature. Parameswaran et al.[13] stated that for the cirrus covered region, the decrease in the environmental lapse rate could possibly be attributed to the cloud induced IR heating. Also, according to Krishnakumar et al.[14], there is a clear correlation between the crystal morphology in the clouds and the dynamical conditions of the prevailing atmosphere. Thus, the ice composition and the microphysics of cirrus can be understood using the lidar data on their scattering properties.

In the present work, these parameters are studied at the tropical station, Gadanki (13.5°N, 79.2°E), India during two different seasons, namely the summer (March, April, May) and the southwest monsoon (June, July, August) during 2006-2010, utilising the data from both the ground and satellite based lidars and are compared with the previously reported results.

2 Instrumentation

2.1 Ground-based lidar

A pulsed monostatic lidar system was set up at the National Atmospheric Research Laboratory (NARL), Gadanki (13.5°N, 79.2°E), India in 1998 in collaboration with Communication Research Laboratory, Japan for the study of atmospheric aerosols and thermal structure of stratosphere and mesosphere[10]. The lidar transmitter at NARL employs an Nd:YAG laser, which emits the laser radiation (frequency doubled) at wavelength 532 nm with an energy of 550 mJ per pulse (pulse-width 7 ns and repetition rate 20 Hz). The laser beam is expanded using a 10x beam expander, which makes the beam divergence < 0.1 mrad. The receiver optics consists of a Schmidt-Cassegrain type telescope with 350 mm diameter and FOV of 1 mrad. The data obtained from the receiver, which operates in the altitude range of 8-20 km, is used for this study. Main technical parameters of this Lidar system are depicted in Table 1.

2.2 Satellite-based lidar

Cloud-Aerosol Lidar and Infrared Pathfinder Satellite Observations (CALIPSO) is a joint NASA-CNES satellite mission designed to provide insight into understanding the role of aerosols and clouds in the climate system on a global scale[15]. The space borne lidar CALIOP on-board the CALIPSO satellite provides high resolution observations, which furnish information on the vertical distribution of aerosols and clouds as well as their optical properties over the globe with high spatial resolution, since June 2006 (Ref. 16). The appropriate inversion algorithms are used to analyse the optical and physical properties of clouds by analysing the dual wavelength and depolarized lidar signals from CALIOP[16]. More about the inversion methods, feature detection, determination of layer properties and the associated uncertainties are detailed in the CALIOP algorithm theoretical basis document[17]. Validation of CALIPSO data with ground-based lidar measurements is essential to the production of a high quality dataset[15]. The technical parameters of CALIOP lidar system are shown in Table 2. For the present study, level 2, 5 km cloud layer and cloud profile (version 3) data products obtained from CALIOP on-board CALIPSO for a grid (5°N - 20°N; 60°E - 85°E) during June 2006 - December 2010 are used. This data consist of layer data with horizontal resolution of 5 km and a vertical

Table 1 — Specifications of ground-based Lidar system

Transmitter

Laser Type	Nd:YAG
Wavelength	532 nm
Average energy per pulse	600 mJ
Average output power	30 W
Pulse width	7 ns
Pulse repetition rate	50 Hz
Beam divergence	0.1 mRad
Beam size	8 mm
Line width	1 cm^{-1}

Receiver

Telescope	Schmidt Cassegrain
Diameter	350 mm
Field of view	1 m rad
Filter	1.13 nm
Filter Transmission	100 %

Detector

PMT	Hamamstu R3234.01

Data acquisition system

Hardware	Multi Channel Scaler Card 1024channels
Range resolution	300 m
Integration time	250 s

Table 2 — Specifications of CALIPSO Lidar system

Laser type	Nd:YAG, diode-pumped, Q-switched, frequency doubled
Wavelength	532, 1064 nm
Average energy per pulse	110 mJ/channel
Pulse repetition rate	20.2 Hz
Receiver diameter	0.1 m
Field of view (m rad)	100 m / 130 μrad
Vertical resolution	30 - 60 m
Horizontal resolution	333 m
Linear dynamic range	22 bits
Data rate	316 kbps

CALIOP spatial resolution of down linked data

Altitude range, km	Horizontal resolution, km	Vertical resolution, m
30.1 - 40.0	5.0	300
20.2 - 30.1	1.67	180
8.2 - 20.2	1.0	60

resolution of 300 m. The ground-based lidar observations are obtained for 108 different nights of the two seasons (summer and southwest monsoon) during 2006 - 2010. In order to obtain useful comparison with the NARL lidar data, the nearest night-time CALIOP overpass observations at Gadanki are considered for the present study. Because of the 16 days repeat cycle of the CALIOP, limited night-time overpasses can be obtained during the observation period and data files are collected in the region selected around Gadanki. However, combined studies with ground-based lidar together with satellite observations allow full exploitation of the data for a detailed description of the temporal and spatial distribution and evolution on a global scale. For the present study, all the temperature data for the ground-based analysis are obtained from the radiosonde observations obtained near the Gadanki station available with Wyoming Atmospheric Data Centre.

3 Data analysis and Methodology

The laser pulse penetrates through the cirrus completely and the signal transition from the top of the cirrus to the clear air can be observed from the data. But the effect of cirrus on retrieving aerosol extinction beyond the cloud is minimal. Also, the presence of clouds is further determined and analysed by deriving the volume extinction coefficient and backscattering coefficient. The lidar system installed at Gadanki station has been operated for three hours in the pre-midnight period regularly since 1998 subject to sky conditions and system integrity. It has also been aligned to an over-lap height of greater than 4 km so as to avoid the intense backscattered signals

from the low altitude clouds and aerosols. Since the high altitude cirrus clouds are mostly thin, their optical attenuation is weak. Fernald inversion method[18] is used to obtain the altitude profiles of the extinction coefficient. Cloud extinction is strictly a combination of macrophysical and microphysical parameters as it is derived from both the physical extent of the cloud, as well as its absorption and scattering characteristics.

The fundamental lidar equation is:

$$P(\text{r}) = P_0 C \tau / 2 \frac{\beta(\text{r})}{\text{r}^2} A \exp\left\{-\int_0^\text{r} \alpha(\text{r})\text{c}\right. \qquad \dots (1)$$

where, P_0 is the transmitted laser power; c, the velocity of light; τ, the laser pulse width; r, the range of the scattering volume from the lidar; A, the effective area of the receiving telescope; $\beta(\text{r})$, the integrated volume backscatter function (expressed in $\text{m}^{-1}\,\text{sr}^{-1}$); and $\alpha(\text{r})$, the integrated volume extinction function (expressed in m^{-1}) of the atmosphere.

Fernald's inversion method[18] is used to inverse the Mie signal which relies on the idea that both backscattering coefficient β and extinction coefficient $\alpha(\text{r})$ in Eq. (1) are from molecules and aerosols of atmosphere, respectively.

The back scattering ratio, R, is defined as:

$$R(\text{r}) = \frac{\beta_\text{m}(\text{r}) + \beta_\text{a}}{\beta_\text{m}(\text{r})} \qquad \dots (2)$$

where, β_a and β_m, are the backscatter coefficients of aerosol and molecules, respectively. Optical depth is a crucial parameter concerning the radiation and scattering processes of the cloud and depends on the composition and thickness of the cloud. Cloud optical depth (COD, τ_c) is calculated by integrating the extinction coefficient from cloud base to its top as:

$$\tau_\text{c} = \int_\text{rbase}^\text{rtop} \alpha(\text{r})\text{d}\text{r} \qquad \dots (3)$$

where, $\alpha(\text{r})$, is the cloud extinction. The following estimations of τ are obtained by Sassen *et al.*[19] from their visual appearance: $\tau_\text{c} \leq 0.03$ for sub visible, $0.03 < \tau_\text{c} \leq 0.3$ for thin, and $\tau_\text{c} > 0.3$ for dense cirrus clouds.

The depolarisation ratio $\delta(\text{r})$, within the cloud is an indicator of cloud microphysical properties and can be obtained from the perpendicular and parallel lidar returns obtained from the P and S channels by Eq. (2). The depolarization ratio is zero for spherical particle. Cirrus clouds, especially over tropics, are mostly

composed of non-spherical ice crystals and cause significant depolarisation.

$$\delta(r) = \delta m \frac{Rs(r)}{Rp(r)} \qquad \ldots (4)$$

where, $Rs(r)$ and $Rp(r)$, are the effective backscatter ratio of the S and P channels, respectively. The molecular depolarisation δm for dry air is assumed to be 0.028 by Bodhaine et al.[20]. This parameter is used to derive the phase of the cloud and thereby to identify the type of ice crystals present within the cloud.

The extinction-to-backscatter ratio, usually called as lidar ratio LR, is an important parameter to obtain the nature of the cloud particles while studying their optical properties. The altitude dependent LR values are obtained from the method described in detail by Satyanarayana et al.[21].

Figure 1 shows typical profiles of received signal in photon counts (a); and retrieved cirrus and aerosol extinction using Fernald method (b).

For CALIPSO observations, only cloud-aerosol discrimination (CAD) score in the range 70-100 and altitude above 8 km are taken for the present study to confirm that all the observed clouds are cirrus in nature.

4 Results and Discussion

4.1 Macro physical characteristics

The vertical distribution of the properties of the cloud derived from the observed data is shown through Figs 2-4. Figure 2 shows the yearly variation of cloud base and top height during the observational period when measured with both ground based and satellite based systems. It indicates that the peak

altitude of the cirrus ranges 8 - 20 km and this is in agreement with Krishnakumar et al.[14]. Also, the top altitudes of some of the clouds are found to be near to the tropopause region.

During summer, from the ground-based lidar observations, it is noted that the clouds occurr in the 13-15 km altitude range on most of the days and in about 70% of the cases, the cloud top height is above 15 km. The average height of the local tropopause during summer season is about 17.5 km. During the southwest monsoon season, the altitude range of the clouds is between 10 and 17 km and the local tropopause has an average height of 16.84 km. In most of the days, the cloud base height is found to be in the range 12 - 16 km, which signifies the occurrence of cloud base within the tropopause vicinity.

In most of the cases, the cloud base is at 14 km during the summer season, but the average height of cloud base during southwest monsoon is 12 km. Large variation observed in the altitude of clouds is normally due to the turbulence below the cloud[14,22]. Parameswaran et al.[22] and Krishnakumar et al.[14] substantiated the role of turbulence in governing the cloud height and shape.

As for the seasonal variability of both the peak altitude of the cirrus and the tropopause height, the former tended to be nearer to the latter, which is in agreement with Wang et al.[11]. In both the seasons, most of the cirrus clouds' top heights observed are 0.8 km above or below the tropopause and the maximum top height occurred during monsoon months. It shows the strength of the tropical convective processes.

The CALIPSO observations during this period show that the clouds have top height between 13 and
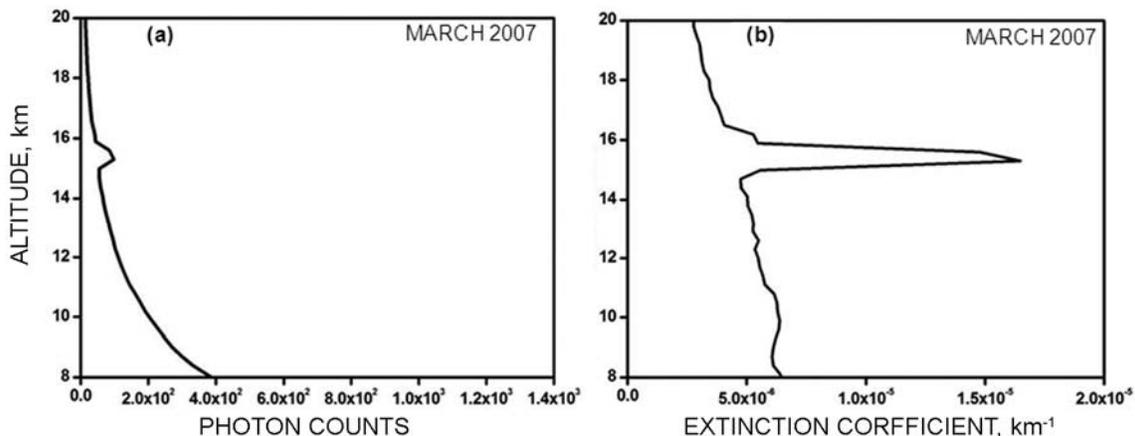
Fig. 1 — Profiles of: (a) lidar received signal; and (b) retrieved cirrus and aerosol extinction using Fernald method
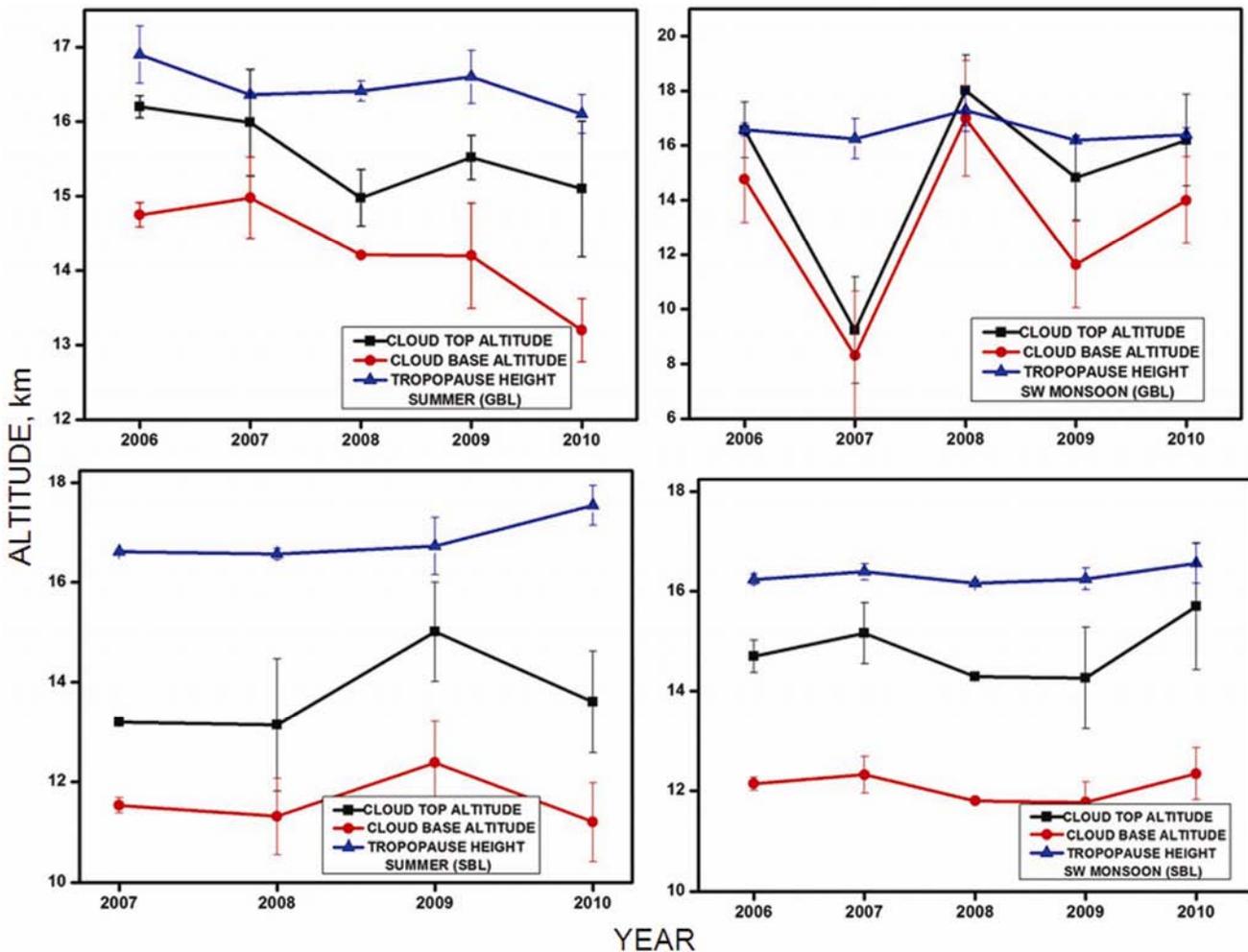
Fig. 2 — Variation of cloud top and base altitudes during the two observed seasons of ground-based lidar (GBL) and satellite-based lidar (SBL) [vertical bars indicate standard deviation]

15.5 km and the base heights is in the range of 11 - 12.5 km. The average tropopause height observed by satellite measurements during this season is 16.86 km. During the southwest monsoon period, most of the clouds are located between 11 and 15.7 km and the average tropopause height is about 16.32 km. The tropopause layer showed the common behaviour of high altitude in summer with high mean mid cloud temperature. Similar to the ground-based measurements, CALIPSO observations also showed a high tropopause altitude during the summer.

Figure 3 shows the annual variation of mid cloud temperature during the two seasons corresponding to ground-based and CALIPSO observations. It is observed that the mid cloud temperature is between –60 and –75°C in most of the cases. This is in agreement with the findings of Rosenfield *et al.*[23], who reported that background temperature for the

formation of cirrus at tropics is between -73 and -76°C and ice crystals normally occur in these clouds. As in Fig. 3(c), the satellite observations show that the average mid cloud temperature during the summer season and southwest monsoon is -49.53°C and -59.12°C, respectively.

Figure 4 depicts the variation of cloud thickness during the period of study. It can be seen that thickness ranges 1 - 3 km, which is in agreement with the data reported earlier for different geographical locations[10]. It also indicates that most of the high altitude cirrus is thin. The convection activity prevailing during this period induces aerosol mixing processes and the density decreases with altitude. This decrease in density reduces the number of nuclei available for cloud condensation, which in turn reduces the cloud thickness[13,14]. The thin cirrus cloud observed have thickness in the range 0.6 - 1.5 km,
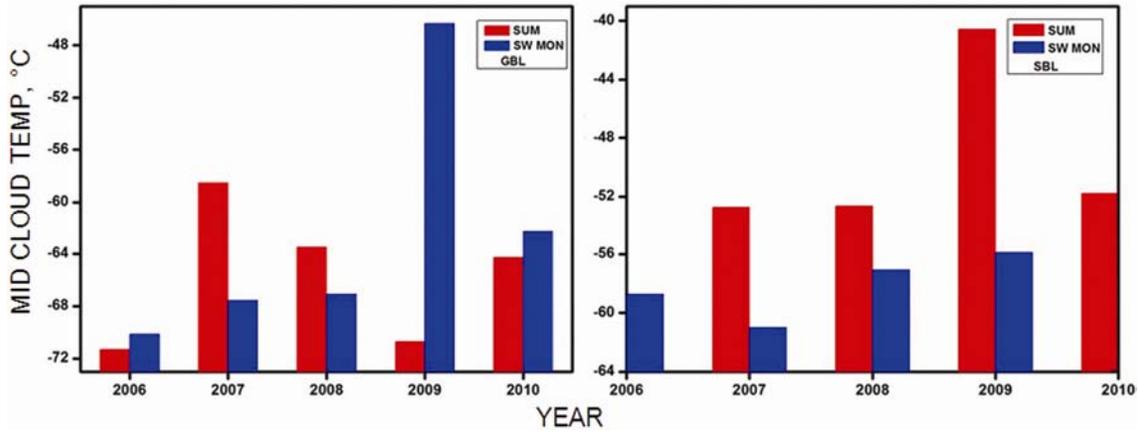
Fig. 3 — Variation of mid cloud temperature of ground-based lidar (GBL) and satellite-based lidar (SBL) during the two seasons
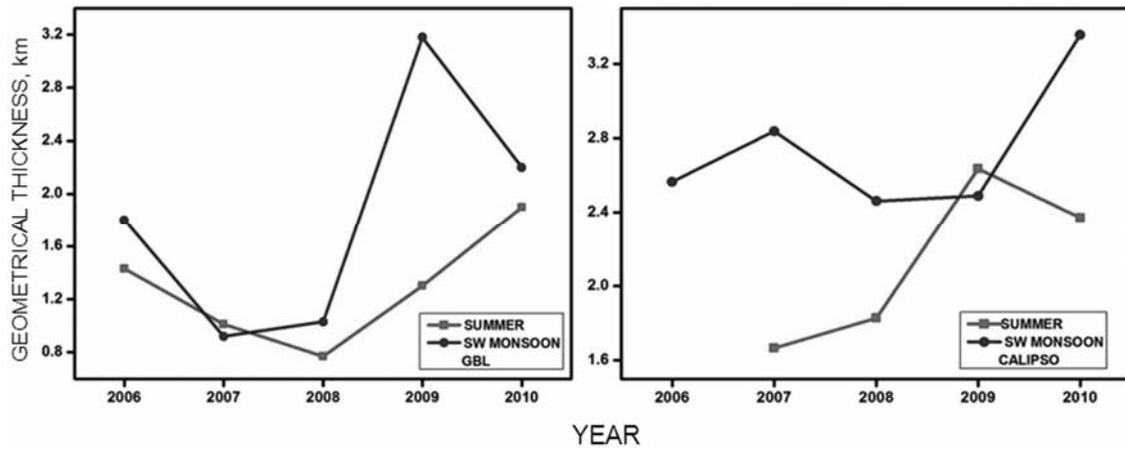
Fig. 4 — Variation of average cloud thickness of ground-based lidar (GBL) and satellite-based lidar (SBL) during the two seasons

whereas for the thick clouds, the range is 1 - 3 km (Ref. 13).

During summer, the average geometrical thickness of the clouds is about 1.33 km. It is noted that 66% of the clouds observed are thin, and the remaining 34% are dense. But during the southwest monsoon season, the average geometrical thickness is about 1.91 km. More than 50% of the clouds observed are dense and about 33% of the clouds are thin. The cloud thickness increases during the southwest monsoon period. Similar variation is observed in the satellite measurements. The average value of cloud geometrical thickness during the summer period is 2.12 km and that of southwest monsoon is 2.74 km.

4.2 Optical properties

4.2.1 Optical depth

Optical depth of a cloud denotes the integrated extinction coefficient for the entire cloud region.

Figure 5 shows the variation of optical depth of the cirrus clouds as derived from ground-based and space borne system. It can be seen that in 66% of the cases, the observed cirrus are sub-visual with τ_c <0.03 and in the 33% of cases, the clouds are thin with 0.03 <τ_c <0.3. It is observed that the cloud optical depth shows peak values during the southwest monsoon period. The convective activity is high at tropics during the monsoon period. The observed variability in optical depth depends on the composition and thickness of the cloud. It is observed that the optical depth increases with the thickness of the cloud. However, due to changes in the microphysical properties when the cloud thickness is quite large, variations are observed in the optical depth. The CALIOP results also agree with the above findings. It is also observed that during monsoon, the optical depth shows an average value of 0.68 and is higher than that obtained during summer season.
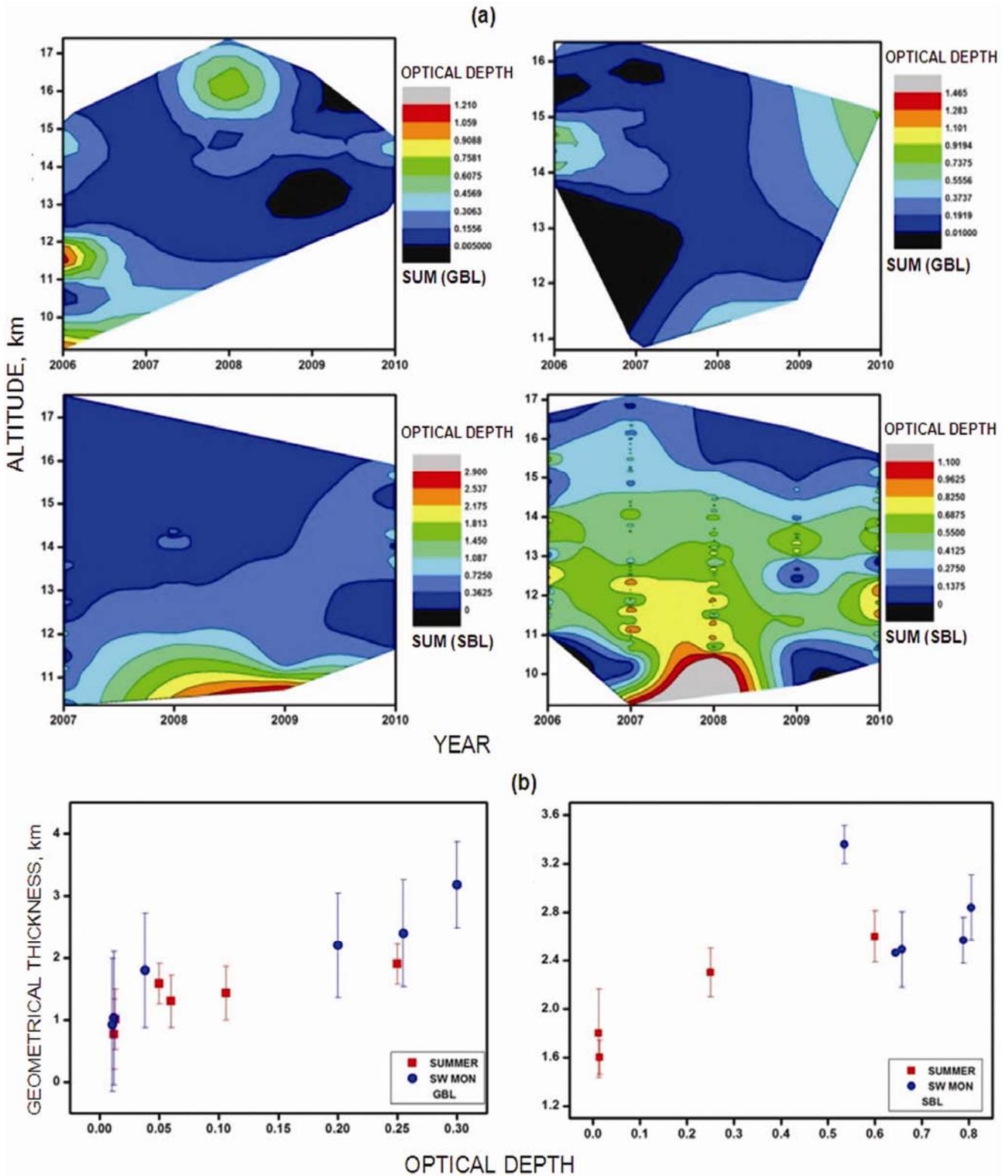
Fig. 5 — (a) Contour plot of seasonal variation of optical depth in two distinct seasons during 2006-10 with ground-based lidar (GBL) and satellite-based lidar (SBL); and (b) its variation with geometrical thickness [vertical bars indicate standard deviation]

In the present study, the optical depth is found to be high when the temperature is between -60°C and -70°C with values around 0.2 to 0.6 as derived from the ground based system. Seasonal variation of cirrus physical properties and optical depth along with the occurrence temperature are shown in Table 3. The CALIPSO observations show that the temperature is between -50°C and -62°C with optical depth values from 0.5 to 0.8. The temperature dependence of the optical depth is shown in Fig. 6. As the temperature rises, optical depth also increases. In summer, the clouds are usually observed very near to the tropopause and hence, the chances for the formation of regular ice crystals are high. But in the other seasons, the conditions are favourable for the occurrences of low altitude clouds are high. In such clouds, the influence of atmospheric turbulence is high leading to decrease of precipitation from the clouds.

4.2.2 Depolarisation ratio

Depolarization measurements are slightly affected by the presence of multiple scattering when a lidar is used to probe the clouds. Fluctuation in the depolarisation ratio indicates the inhomogeneity of cloud particles. The water droplets generate almost negligible depolarisation of incident laser light in the exact backscattering direction, whereas the ice crystals generate a significant depolarisation. Depolarisation values above 0.50 are associated with dust and ice particles.

Figure 7 shows the contour plot of altitude variation of depolarisation during the seasons obtained using the two lidar techniques. The depolarisation ratio values vary between 0.1 and 0.4 in most of the cases and show slightly increasing tendency at high altitudes. It can be clearly seen that during the summer seasons, there is a slight increase in depolarisation ratio near the tropopause region.

Table 3 — Seasonal variation in the geometrical and optical thickness of cirrus clouds along with their location and temperature during 2006-2010 from ground-based observations

Year	Season	Cloud top height, km	Cloud base height, km	Geometrical thickness, km	Tropopause height, km	Optical depth
2006	Summer	17.20	15.76	1.43	14.3	0.106
	SW monsoon	16.57	14.76	1.80	16.58	0.038
2007	Summer	15.99	14.98	1.01	16.36	0.0139
	SW monsoon	9.24	8.31	0.92	16.25	0.0106
2008	Summer	14.98	14.20	0.77	13.41	0.012
	SW monsoon	19.02	17.99	1.03	15.70	0.0118
2009	Summer	15.52	14.2	1.3	16.6	0.6
	SW monsoon	14.82	11.64	3.18	16.20	0.3
2010	Summer	15.10	13.2	1.9	16.1	0.25
	SW monsoon	16.2	14	2.2	16.4	0.2
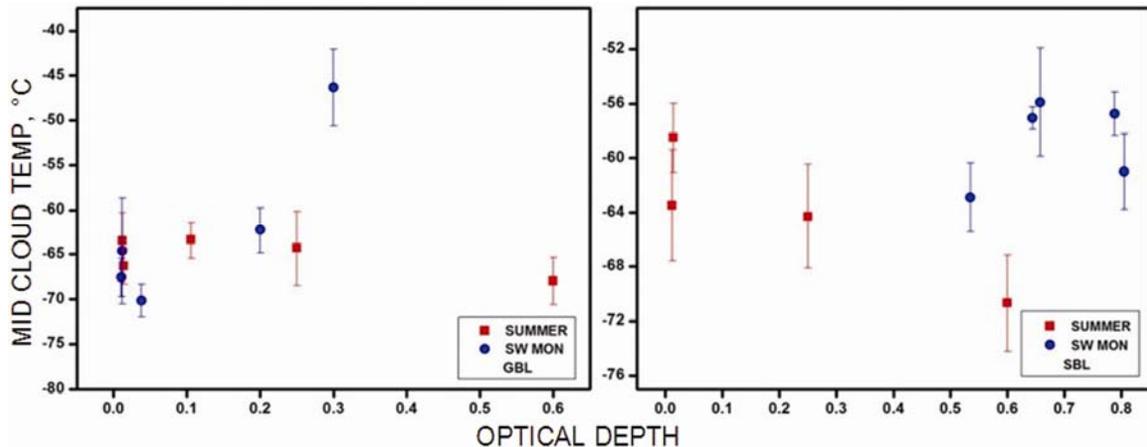
Fig. 6 — Variation of optical depth with respect to the mid cloud temperature with ground-based lidar (GBL) and satellite-based lidar (SBL) during the two seasons [vertical bars indicate standard deviation]

From the satellite observations, it is seen that the average depolarisation ratio shows higher values during southwest monsoon than summer.

Figure 8 represents the temperature dependence of depolarisation ratio and it shows a negative dependence. The depolarisation values tend to increase with decrease in temperature. The mid cloud temperature of cirrus clouds at higher altitudes is low and the ice-crystal content is high, which in turn increases the depolarization[11].
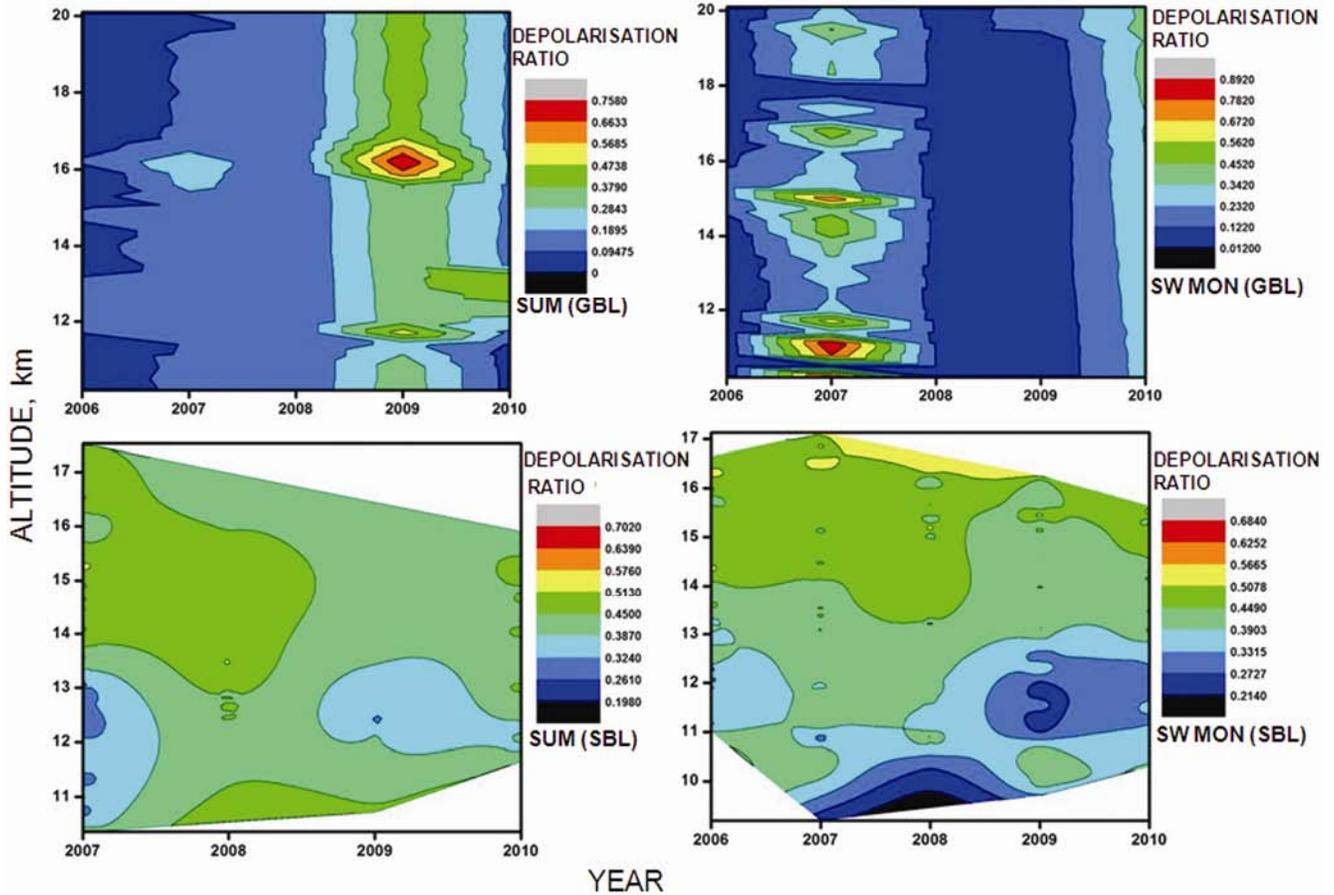
Fig. 7 — Contour plot of seasonal variation of depolarisation ratio of two distinct seasons during 2005-10 with ground-based lidar (GBL) and satellite-based measurements (SBL)
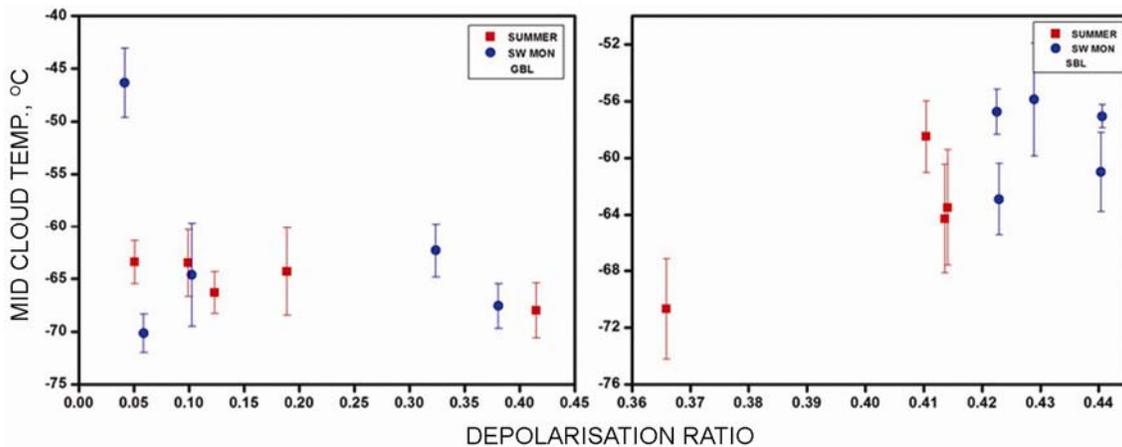
Fig. 8 — Dependence between average depolarisation ratio and corresponding temperature with ground-based lidar (GBL) and satellite-based lidar (SBL) during the two seasons [vertical bars indicate standard deviation]

4.2.3 Lidar ratio

The lidar ratio (LR) is a key parameter in deriving the microphysical properties and the structure of the cirrus in the corresponding height region[24]. Figure 9 shows the contour plot of seasonal variation of lidar ratio during the period of observation. Above 12 km, the lidar ratio values are mainly distributed in the range of 20-30 sr in most of the cases for both observation techniques. During summer periods, LR values are in the range 15-57 sr; and in monsoon, LR varies between 20 and 37 sr and shows relatively higher values (~25-30 sr) throughout the observation period. By the CALIPSO observation, LR values vary between 24 and 35 sr during summer; and between 24 and 95 sr during southwest monsoon. The calculated lidar ratio can be compared with the earlier studies of cirrus. Seifert et al.[25] studied tropical cirrus cloud over Maldives on the basis of northeast and southwest monsoon and derived a mean lidar ratio of 32±10 sr.

Das et al.[26] determined the effective lidar ratio using the simulation of lidar backscatter signals, which varies from 1 to 77 sr with a mean value of 23±16 sr statistically. These results are in agreement with the findings of the present study. All the discussed statistics of the microphysical properties of cirrus clouds obtained by the ground-based lidar system over the tropical station Gadanki are presented in Table 3.

Figure 10 gives the relationship between lidar ratio and mid-cloud temperature. It can be seen that the lidar ratio varies with mid-cloud temperature with no clear tendency with both the observation techniques. This may be due to the variations in the ice crystal properties even at the same temperature range or may be due to the heterogeneous cirrus formations over the region[27]. But in some cases, the high LR values observed at lower temperature region indicates the presence of thin cirrus clouds.
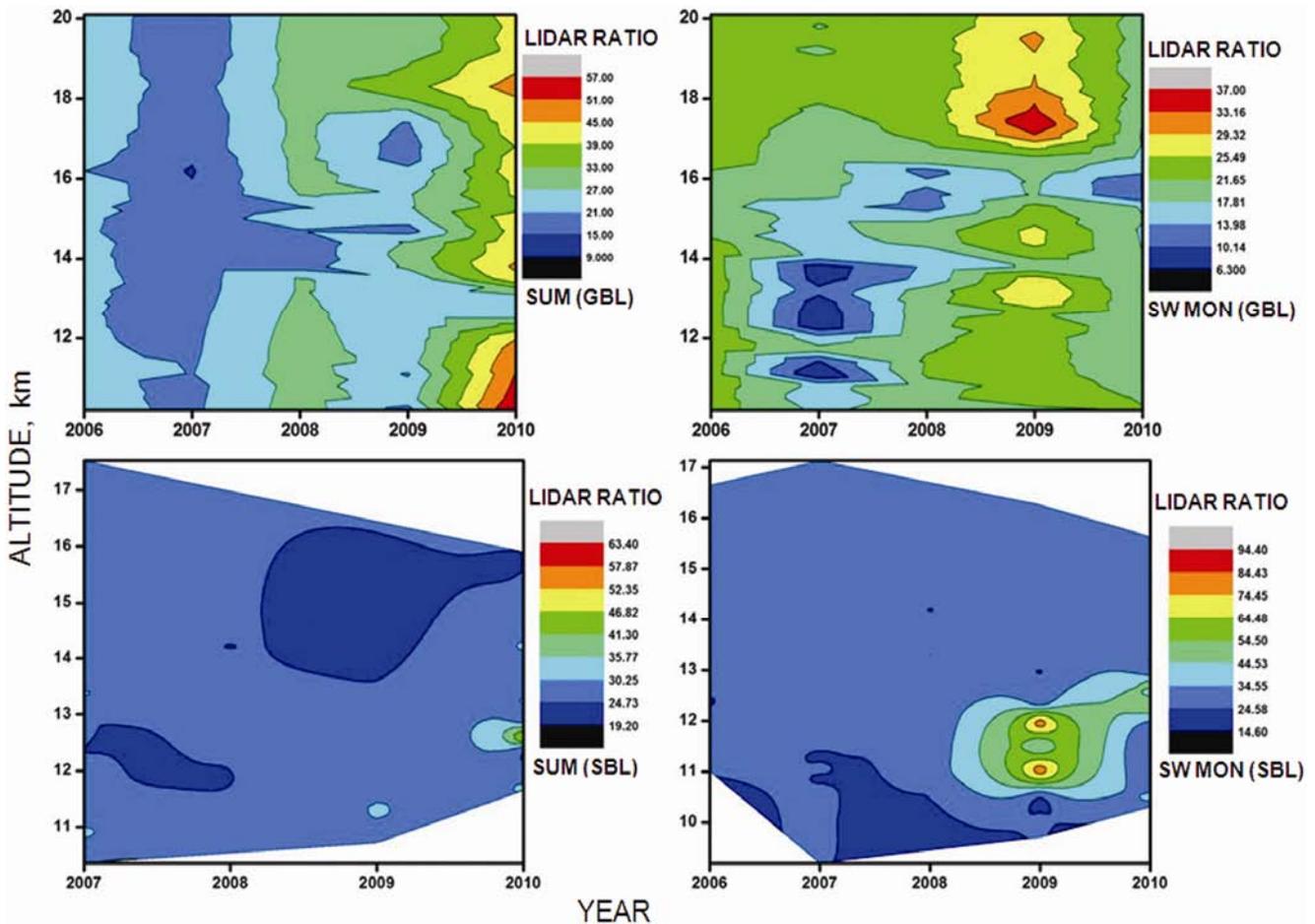
Fig. 9 — Contour plot of seasonal variation of lidar ratio of two distinct seasons during 2006-10 with ground-based lidar (GBL) and satellite-based measurements (SBL)
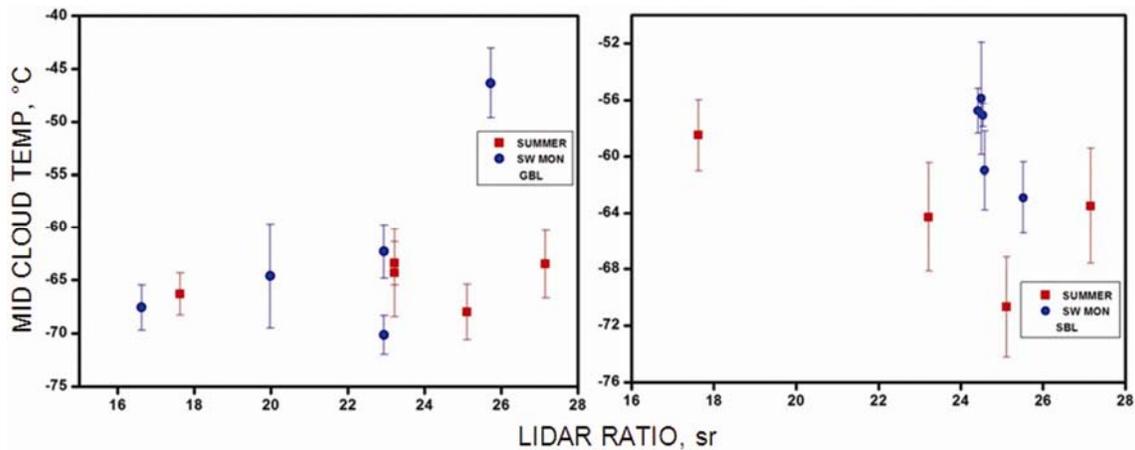
Fig. 10 — Dependence between average lidar ratio and corresponding temperature with ground-based lidar (GBL) and satellite-based lidar (SBL) during the two seasons [vertical bars indicate standard deviation]

5 Conclusion

The mean physical and optical properties of tropical cirrus clouds at night time during the two contrasting periods, viz. the southwest monsoon period (June, July and August) and summer period (March, April and May) during the years 2006 - 2010 are investigated using the ground-based lidar system over the tropical station, Gadanki (13.5°N,79.2°E), India. The cirrus properties are also derived from the space based lidar CALIOP for comparison. The properties derived from the ground and space based lidar observations broadly match to a large extent. However, small differences are noticed as the observations are not obtained exactly at the same place and the sampling frequencies are also different. A statistical analysis of both macro-physical and microphysical characteristics has been done for the observations from the two measurement systems. Some of the general observations from the results are :

- Cirrus cloud layers are situated within 8−20 km altitude range with the atmospheric temperatures ranging from -40 to -80°C and mostly are located very close to the tropopause. The peak altitudes of most of the observed cirrus clouds are found to be in the vicinity of the tropopause.
- The mid-cloud temperature of most of the observed cirrus varied from -60 to -75°C with an average tropopause height of 16.5 km. Both the parameters show high values during the summer season.
- The cirrus geometrical thickness ranges 0.8 - 3 km and shows an increasing tendency during southwest monsoon period.

- The optical depth is in the range 0.02 - 2.5 and shows higher values during the southwest monsoon than summer. The optical depth increases with the geometrical thickness of the clouds. The optical depth shows a negative correlation with the mid-cloud temperature.
- The depolarization ratio of cirrus clouds varies from 0.1 to 0.4 and shows slightly increasing tendency with high altitudes associated with lower temperatures. The wide range of depolarization ratio suggests the presence of various forms of non-spherical ice particles. The height dependence of depolarization ratio shows that cirrus clouds may have various compositions of ice particles at any particular altitude.
- The lidar ratio varies from 10 to 60 sr with no clear tendency with altitude and temperature.
- The satellite based lidar measurements mostly match with the ground-based lidar values except in few cases, which is attributed to the large swath covered by the CALIOP lidar on-board the CALIPSO satellite.

References

1   Liou K N, Influence of cirrus clouds on weather and climate processes: A global perspective, *Mon Weather Rev (USA)*, 114 (6) (1986) pp 1167-1192, doi.org/10.1175/1520-0493.

2   Fu Q & Liou K N, Parameterization of the radiative properties of cirrus clouds, *J Atmos Sci (USA)*, 50 (1993) pp 2008-2025.

3   Lynch.D K, Sassen K, Starr D O & Stephens G: Eds, *Cirrus* (Oxford Univ Press, New York), 2002, 480.

4   Stephans G L, Tsay S C, Stackhouse Jr W S & Flatau P J, The relevance of the microphysical and radiative properties of cirrus clouds to climate and climatic feedback, *J Atmos Sci (USA)*, 47 (14) (1990) pp 1742-1754, doi: 10.1175/15200469.

5   Liou K N & Takano Y, Interpretation of cirrus cloud polarization measurements from radiative transfer theory, *Geophys Res Lett (USA)*, 29 (2002), doi: 10.1029/2001GL014613.

6   Fierli F, Di Donfrancesco G, Cairo F, Marecal V, Zampieri ´M, Orlandi E & Durry G, Variability of cirrus clouds in a convective outflow during the Hibiscus campaign, *Atmos Chem Phys (Germany)*, 8 (2008) pp 4547-4558.

7   Jensen E J, Pfister L, Ackerman A S & Tabazadeh A, A conceptual model of the dehydration of air due to freeze drying by optically tin laminar cirrus rising slowly across the tropical tropopause, *J Geophys Res (USA)*, 106 (2001) pp 17273-17252.

8   Gettelman A, Randel W J, Wu F & Massie S T, Transport of water vapour in the tropical tropopause layer, *Geophys Res Lett (USA)*, 29 (2002) 1009, doi: 10.1029/2001GL013818.

9   Wang X, Boselli A, Avino L D, Velotta R, Spinelli N, Bruscaglioni P, Ismaelli A & Zaccanti G, An algorithm to determine cirrus properties from analysis of multiple-scattering influence on lidar signals, *Appl Phys B (Germany)*, 80 (2005) pp 609-615.

10 Sunilkumar S V & Parameswaran K, Temperature dependence of tropical cirrus properties and radiative effects, *J Geophys Res (USA)*, 110 (2005) D13205.

11 Wang Zhen Zhu, Chi Ruli, Liu Bo & Zhou Jun, Depolarization properties of cirrus clouds from polarization lidar measurements over Hefei in spring, *Chin Opt Lett (China)*, 6 (2008) pp 235-237.

12 Sivakumar V, Bhavanikumar Y, Rao P B, Mizutani K, Aoki T, Yasui M & Itabe T, Lidar observed characteristics of the tropical cirrus clouds, *Radio Sci (USA)*, 38 (6) (2003) 1, doi: 10.1029/2002RS002719.

13 Parameswaran K, SunilKumar S V, Murthy B V K, Satheesan K, Kumar Y B, Krishnaiah M & Nair P R, Lidar observations of cirrus cloud near the tropical tropopause: Temporal variations and association with tropospheric turbulence, *Atmos Res (USA),* 69 (1–2) (2003) pp 29-49, doi.org/10.1016/j.atmosres.2003.08.002.

14 Krishnakumar V, Satyanarayana Malladi, Dhaman Reji K, Radhakrishnan S R, Jayeshlal G S, Motty G S, Mahadevan Pillai V P, Raghunath K, Venkata Ratnam M, Ramakrishna Rao D & Sudhakar P, Lidar investigations on the optical and dynamical properties of cirrus clouds in the upper troposphere and lower stratosphere regions at a tropical station, Gadanki, India (13.5°N, 79.2°E), *J Appl Remote Sens (USA)*, 8 (1) (2014) 083659, doi: 10.1117/1.JRS.8.083659.

15 Winker D M, Hunt W H & McGill M J, Initial performance assessment of CALIOP, *Geophys Res Lett (USA)*, 34 (19) (2007) L19,803, doi: 10.1029/2007GL030135.

16 Meenu S, Rajeev K & Parameshwaran K, Regional and vertical distribution of semi-transparent cirrus clouds and cloud top altitudes over tropical Indian region derived from CALIPSO data, *J Atmos Sol-Terr Phys (UK)*, 73 (13) (2011) pp 1967-1979, doi: 10.1016/j.jastp.2011.06.007.

17 Vaughan M, Winker D & Powell K, *CALIOP algorithm theoretical basis document Part 2: Feature detection and layer properties algorithms*, PC-SCI-202 Part 2, Release 1.01 (NASA Langley Research Centre, Hampton, VA), 2005.

18 Fernald F G, Analysis of atmospheric lidar observations: some comments, *Appl Opt (USA)*, 23 (1984) pp 652-653.

19 Sassen K & Cho B S, Sub-visual thin cirrus lidar data set for satellite verification and climatological research, *J Appl Meteorol (USA)*, 31 (11) (1992) pp 1275-1285, doi: 10.1175/1520-0450.

20 Bodhaine B A, Wood B N, Dutton E G & Slusser J R, On Rayleigh optical depth calculations, *J Atmos Ocean Technol (USA)*, 16 (1999) pp 1854-1861.

21 Satyanarayana M, Radhakrishnan S R, Mahadevan Pillai V P, Veerabhuthiran S, Raghunath K, Presennakumar B & Murthy V S, Laser radar characterization of atmospheric aerosols in the troposphere and stratosphere using range dependent lidar ratio, *J Appl Remote Sens (USA)*, 4 (2010) 043503.

22 Parameswaran K, Sunilkumar S V, Krishna Murthy B V, Satheesan K, Bhavanikumar Y, Krishnaiah M & Nair P R, Lidar observations of cirrus cloud near the tropical tropopause: Temporal variations and association with tropospheric turbulence, *Atmos Res (USA)*, 69 (2003) pp 29-49.

23 Rosenfield J E, Considine D B, Schoeberl M R & Browell E V, The impact of sub-visible cirrus clouds near the tropical tropopause on stratospheric water vapor, *Geophys Res Lett (USA)*, 25 (1998) pp 1883-1886.

24 Heymsfield A J & Platt C M R, A parameterization of the particle size spectrum of ice clouds in terms of ambient temperature and their ice water content, *J Atmos Sci (USA)*, 41 (1984) pp 846-855, doi: 10.1175/1520-0469.

25 Seifert P, Ansmann A, Muller D, Wandinger U, Althausen D, Heymsfield A J, Massie S T & Schmitt C, Cirrus optical properties observed with lidar, radiosonde, and satellite over the tropical Indian Ocean during the aerosol polluted northeast and clean maritime southwest monsoon, *J Geophys Res (USA)*, 110 (2007) D13205, doi: 10.1029/2004JD005426.

26 Das S K, Chiang C W & Nee J B, Characteristics of cirrus clouds and its radiative properties based on lidar observation over Chung-Li, Taiwan, *Atmos Res (USA)*, 93 (4) (2009) 723, doi: 10.1016/j.atmosres.2009.02.008.

27 Sassen K & Cho B S, Sub-visual thin cirrus lidar data set for satellite verification and climatological research, *J Appl Meteorol (USA)*, 31 (11) (1992) pp 1275-1285, doi: 10.1175/1520-0450.